Identification of excited states in ^{117}Cs: Systematics of the $\nu(h_{11/2})^2$ alignment

J. F. Smith,[1,2,*] V. Medina-Chico,[1] C. J. Chiara,[2] D. B. Fossan,[2] G. J. Lane,[2,†] J. M. Sears,[2] I. Thorslund,[2] H. Amro,[3] C. N. Davids,[3] R. V. F. Janssens,[3] D. Seweryniak,[3] I. M. Hibbert,[4,‡] R. Wadsworth,[4] I. Y. Lee,[5] and A. O. Macchiavelli[5]
[1]*Schuster Laboratory, The University of Manchester, Manchester, M13 9PL United Kingdom*
[2]*Department of Physics and Astronomy, State University of New York at Stony Brook, Stony Brook, New York 11794-3800*
[3]*Argonne National Laboratory, Argonne, Illinois 60439*
[4]*Department of Physics, University of York, Heslington, York YO1 5DD, United Kingdom*
[5]*Nuclear Science Division, Lawrence Berkeley National Laboratory, Berkeley, California 94720*
(Received 16 September 2000; published 24 January 2001)

Excited states have been identified in the very neutron-deficient $^{117}_{55}Cs_{62}$ nucleus. High-spin spectroscopy has been performed using the Gammasphere array, and the assignment of gamma-ray transitions to ^{117}Cs has been made in a separate experiment in which gamma rays were detected in coincidence with x rays and with recoiling evaporation residues. A previously observed sequence of five gamma rays has been extended by 11 transitions, to high spin, and has been identified as the yrast $\pi(h_{11/2})[550]1/2^-$ band of ^{117}Cs. Two additional bands have been observed and are tentatively assigned to be based on protons in the $[404]9/2^+$ and $[422]3/2^+$ orbitals. Alignments of pairs of $h_{11/2}$ neutrons and protons are observed in all of the bands. The alignments are compared to cranked Woods-Saxon calculations, and are discussed with respect to the effects of a neutron-proton interaction. Of particular interest are the features of the $\nu(h_{11/2})^2$ alignment in the $\pi[550]1/2^-$ band and of the $\pi(h_{11/2})^2$ alignment in the $[422]3/2^+$ band. The frequencies of these alignments can be qualitatively explained only if a neutron-proton interaction is taken into account.

DOI: 10.1103/PhysRevC.63.024319 PACS number(s): 21.10.Re, 23.20.Lv, 27.60.+j, 29.30.Kv

I. INTRODUCTION

Experimental data show that the very neutron-deficient $A \simeq 120$, $Z = 55$ cesium isotopes are well deformed and display a wealth of interesting collective structures [1–5]. In these nuclei, the cranked shell model (CSM) predicts the rotational alignment of pairs of both neutrons and protons in the $h_{11/2}$ subshell. The precise details of the observed alignments, specifically, the rotational frequency, the gain in aligned angular momentum and the interaction strength, can give information about the structure of the nucleus, particularly when Pauli blocking arguments can be applied. Using such blocking arguments, systematic comparisons with neighboring nuclei, can provide insight into the underlying physics as a function of N and Z. For the neutron-deficient cesium isotopes, CSM calculations predict the interaction strength of the $h_{11/2}$ neutron alignment to oscillate as a function of neutron number. Though experimental data for $^{121-129}$Cs would appear to validate this theory, the data for ^{119}Cs contradict the theory because the interaction strength increases at $N = 64$, suggesting that the interaction strength violates the predicted oscillation by increasing at $N = 64$. In the work by Lidén *et al.* [1], this observation has been presented as evidence for increased neutron-proton interactions between $h_{11/2}$ protons and the $h_{11/2}$ neutrons in the crossing band. In order to test this interpretation, it is necessary to investigate rotational bands and quasiparticle alignments in the cesium isotopes with neutron numbers (N) below 64.

The cesium isotopes with $A < 119$ ($N < 64$) are difficult to study with in-beam spectroscopic techniques, because they can only be produced with very small cross sections from the most neutron-deficient compound nuclei. Until recently the most neutron-deficient cesium isotope in which excited states had been definitively identified was ^{119}Cs [1]. Five transitions, however, had been tentatively assigned to ^{117}Cs by Sun *et al.* in Ref. [6]. In that work, the ^{92}Mo(^{28}Si,$2pn$)^{117}Cs reaction was used; on the basis of statistical-code calculations, excitation-function measurements, and excitation-energy systematics, a band was assigned to ^{117}Cs. The observed band was associated with the yrast $\pi h_{11/2}$ configuration, and reached a spin of $31/2\,\hbar$. The $N = 58$ isotope ^{113}Cs has been studied recently by recoil-decay tagging [7], taking advantage of its decay by proton emission. That work identified a sequence of five gamma rays despite a very small production cross section of $\sim 25\ \mu$b.

In the present work, the isotope ^{117}Cs has been studied, in order to investigate quasiparticle alignments and elucidate general high-spin properties in this very neutron-deficient region. This paper reports the first definite experimental identification of excited states in ^{117}Cs, and the first high-spin spectroscopy of this nucleus. The reactions ^{58}Ni(^{64}Zn,αp)^{117}Cs and ^{64}Zn(^{58}Ni,αp)^{117}Cs have been used, for which the cross sections are only a few mb. High-spin spectroscopy was performed using the Gammasphere [8] array, and the assignment of excited states to ^{117}Cs was made in a separate experiment using the Argonne Fragment

*Corresponding author. Schuster Laboratory, The University of Manchester, Manchester M13 9PL, UK. Tel: (44) 161 275 4155, Fax: (44) 161 275 5509. Electronic address: jfs@mags.ph.man.ac.uk

†Present address: Nuclear Science Division, Lawrence Berkeley National Laboratory, Berkeley, CA 94720.

‡Present address: Oliver Lodge Laboratory, University of Liverpool, Liverpool L69 7ZE, UK.

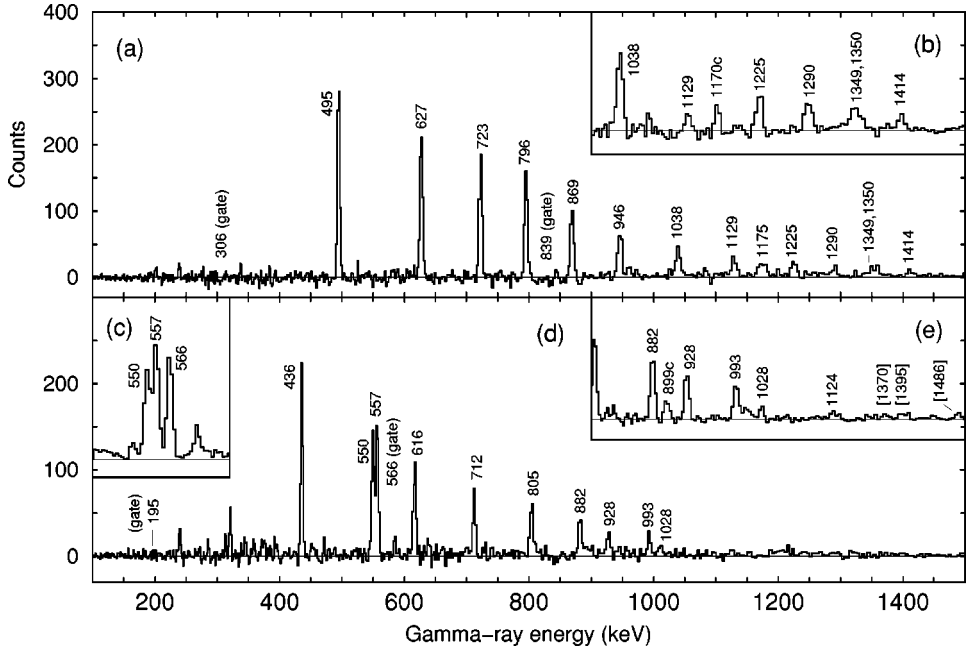

FIG. 1. Representative spectra from the Gammasphere data. The spectra are projected from the $\gamma\gamma\gamma$ coincidence cube by specifying two gating transitions. Panels (a) and (b) show transitions in Band 1 while panels (c), (d), and (e) show transitions in Band 2. The spectra are gated on the following transitions, where all of the given transition energies are in keV: (a) 306 and 839; (b) 306 and (1129 or 1225); (c) 195 and 436; (d) 195 and 566; and (e) (195, 436, 557, 566, or 550) and 712. The peaks are labeled with gamma-ray energies in keV and all of the labeled peaks have been assigned to ^{117}Cs, apart from those labeled with a ''c,'' which are contaminants from neighboring nuclei. The transitions with energies in square brackets on panel (e) could not be definitively shown to be in coincidence with Band 2.

Mass Analyzer (FMA) [9], in which gamma-recoil and gamma-x-ray coincidence events were recorded.

II. EXPERIMENTAL DETAILS AND ANALYSIS

A. The Gammasphere experiment

Details of the experiments have already been given in Refs. [10,11]. In the first experiment, high-spin states were populated using the ^{58}Ni(^{64}Zn,αp)^{117}Cs reaction and de-excitation gamma rays were detected using the Gammasphere array. The 265-MeV ^{64}Zn beam was accelerated by the 88-inch cyclotron at the Lawrence Berkeley National Laboratory. The beam was incident upon two stacked 500-μg/cm^2, self-supporting, 99%-pure ^{58}Ni foils. At the time of the experiment, Gammasphere had 56, 75%-efficient escape-suppressed germanium detectors in place. The detectors were arranged in 14 rings with constant polar angle θ; 2 detectors at $\theta=17.3°$, 5 at 31.7°, 5 at 37.4°, 5 at 50.1°, 1 at 58.3°, 1 at 80.7°, 6 at 90.0°, 1 at 99.3°, 1 at 100.8°, 5 at 121.7°, 10 at 129.9°, 5 at 142.6°, 4 at 148.3°, and 5 at 162.7°. With the requirement that at least three germanium detectors fired in prompt coincidence before data were recorded, a total of 9×10^8 gamma-ray coincidence events were written to magnetic tape. In the offline analysis each n-fold event ($n\geqslant3$) was decomposed into $^nC_3$ threefold gamma-ray coincidences, yielding a total of 6×10^9 unfolded triples which were subsequently used to increment a three-dimensional histogram (cube). The RADWARE software package [12] was used to analyze the data. By gating on known transitions, approximately 15 nuclei were observed. The most intensely populated nuclei were ^{119}Cs ($3p$ evaporation), ^{118}Xe ($4p$), and ^{116}Xe ($\alpha 2p$) which were produced with approximately 33%, 30%, and 19% of the evaporation-residue cross section, respectively. The band assigned to ^{117}Cs in Ref. [6] was observed in the data and two additional bands were tentatively assigned to ^{117}Cs on the basis of systematics, and on the lack of coincidence relationships with level schemes of known nuclei. In total, these bands were populated with about 2–3% of the evaporation-residue yield, corresponding to a cross section of about 5 mb. Figures 1 and 2 show representative spectra projected from the cube by applying gates to two of the three axes of the cube.

B. The ATLAS/FMA experiment

In order to confirm that the bands observed with Gammasphere belonged to ^{117}Cs, a second experiment was performed in which gamma rays were detected in coincidence with recoiling evaporation residues and with x rays. In this experiment, the ^{64}Zn(^{58}Ni,αp)^{117}Cs reaction was used. The ^{58}Ni beam, at energies of 230 and 240 MeV, was provided by the Argonne Tandem Linac Accelerator System (ATLAS). The target was a self-supporting ^{64}Zn foil of thickness 500 μg/cm^2. Gamma rays and x rays were detected at the reaction site in an array of 10 Compton-suppressed, 25%-efficient, germanium detectors; the electronic thresholds on two of the detectors were reduced in order to detect $\sim$35-keV K x rays from nuclei with $Z\simeq55$. The recoiling reaction products were dispersed according to their mass-to-charge state ratio and detected in a parallel-grid avalanche

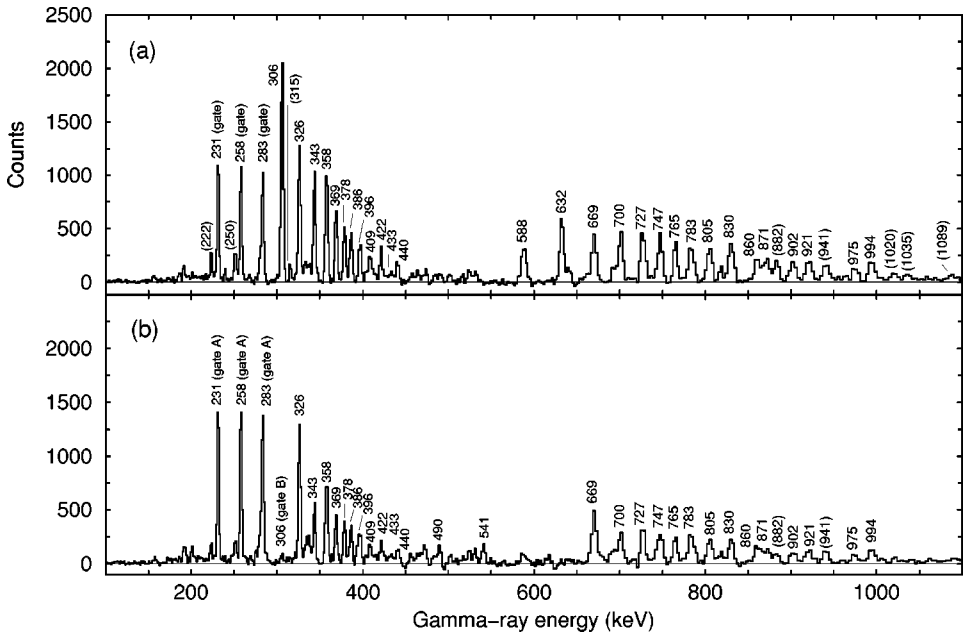

FIG. 2. Representative spectra from the Gammasphere data. Both panels show transitions in Band 3. The spectra are projected from the $\gamma\gamma\gamma$ coincidence cube by specifying two gating transitions. Spectrum (a) is gated on any two of the 231-keV, 258-keV, and 283-keV transitions, that is, the spectrum is a sum of three double gates. The intensities of the gating transitions are clearly reduced. Spectrum (b) is gated on (231, 258, or 283 keV) and 306 keV. The peaks are labeled with the gamma-ray energies in keV and all of the labeled peaks correspond to transitions in ^{117}Cs. The peaks labeled with transition energies in parentheses appear to be in coincidence with Band 3, but could not be placed in the level scheme.

counter (PGAC) at the focal plane of the FMA. With the trigger condition of two or more Ge detector signals in coincidence with each other or one or more Ge signals in coincidence with a PGAC signal, approximately 9×10^7 events were recorded.

C. Assignment of excited states to ^{117}Cs

The M/q spectrum recorded by the PGAC at the FMA focal plane is presented in Fig. 3. Mass (M) 117 recoils with three different charge states (q) were detected by the PGAC; these consisted of ^{117}Xe and ^{117}Cs residues, in approximately equal proportion. The data were sorted into gamma-gamma correlation matrices gated on recoils with masses 115 to 120, and an ungated (no recoil condition) matrix. The method used to assign excited states to ^{117}Cs was essentially the same as that described for ^{118}Ba and ^{118}Cs in Refs. [10,11]. Figure 4(a) shows the total projection of the $M=117$ gated matrix; some of the transitions belonging to ^{117}Cs are labeled with their transition energies on that figure. Figure 4(b) shows gamma rays in coincidence with an $M=117$ recoil and either a 231- or 258-keV gamma ray. The spectrum shows the coincident gamma rays which would be expected from one of the bands identified in the Gammasphere data, and therefore confirms that this band belongs to a nucleus with $A=117$.

Figure 4(c) shows the spectrum projected from the ungated (no recoil requirement) matrix by gating on the 231- or 258-keV transitions; on this figure, the peaks which are labeled belong to the band identified in the Gammasphere data, and these peaks clearly dominate the spectrum. The low-energy (<50 keV) part of this spectrum is shown in Fig. 4(d), showing the K x rays in coincidence with the unidentified band. For comparison, also shown on panel (d) are the low-energy regions of uncontaminated spectra gated on transitions in ^{118}Xe (472 keV) [13], ^{119}Cs (269 keV) [1,14], and ^{119}Ba (113 keV) [15]. The x rays in coincidence with the unidentified band have the same energies as those in coincidence with gamma rays in ^{119}Cs, thus confirming that the band belongs to an isotope of cesium. Hence, these results prove that one of the unidentified bands from the Gammas-

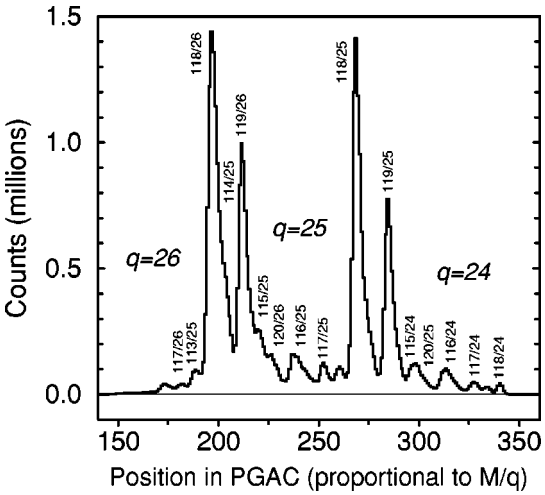

FIG. 3. The spectrum of evaporation residues recorded in the PGAC at the focal plane of the FMA. The peaks are labeled with their values of M/q, the mass to charge-state ratio.

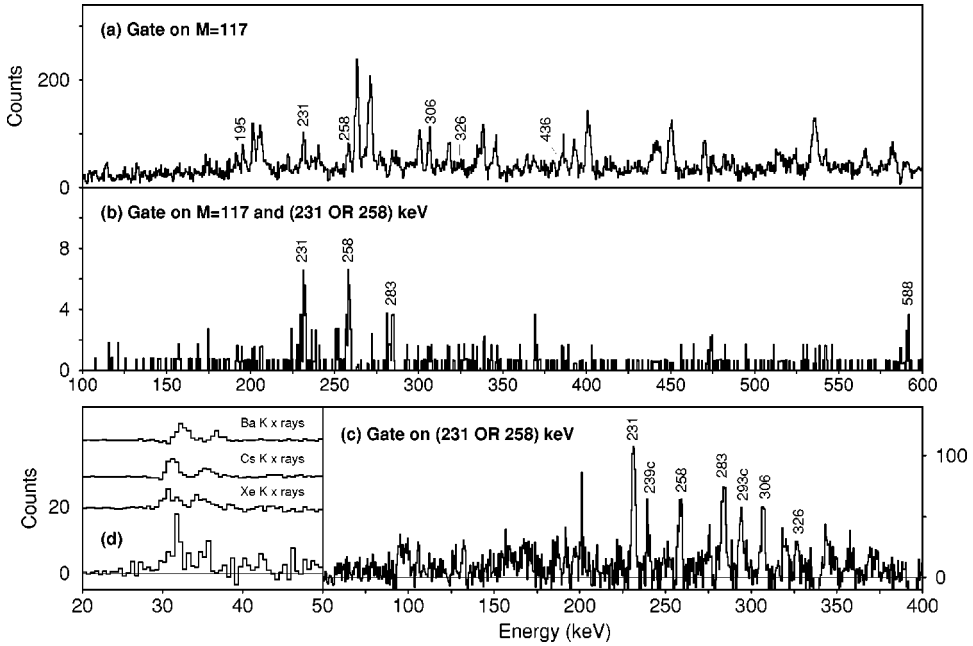

FIG. 4. Spectra from the ATLAS/FMA experiment. Panel (a) shows the total projection of the gamma-gamma matrix gated on $M=117$ recoils. Some of the ^{117}Cs peaks are labeled with their transition energies. Panel (b) shows the spectrum of gamma rays in coincidence with an $M=117$ recoil and a 231- or 258-keV gamma ray. Panel (c) shows the total spectrum of gamma rays in coincidence with either the 231- or 258-keV transitions (the spectrum is not gated on recoils). Again, several of the transitions in ^{117}Cs are marked with their transition energies in keV. The transitions marked by the letter ''c'' after the transition energies are contaminants. The lower spectrum of panel (d) shows the K x-ray region of the spectrum of panel (c). The upper three spectra of panel (d) show the K x-ray regions of spectra gated on known transitions in ^{118}Xe ($Z=54$), ^{119}Cs ($Z=55$), and ^{119}Ba ($Z=56$).

phere data (later labeled Band 3 on Fig. 5) belongs to ^{117}Cs. From this data, it was not possible to confirm the assignment of Band 1 or Band 2 of ^{117}Cs; this will be discussed in Sec. III B and IV A.

III. RESULTS

A. The level scheme of ^{117}Cs

Coincidence relationships, together with energy- and intensity-balance arguments, have been used to deduce the level structures presented in Fig. 5. Three independent rotational bands, labeled Band 1, Band 2, and Band 3, have been observed. No transitions have been seen linking the bands, and as a result their relative spins and excitation energies have not been established. Excitation-energy systematics of the odd-A cesium isotopes, and aligned-angular momentum arguments (which are presented in Sec. IV B) suggest that Band 1 is based on the $\pi(h_{11/2})[550]1/2^-$ orbital, Band 2 on the $\pi(g_{7/2}d_{5/2})[422]3/2^+$ orbital, and Band 3 on a hole in the $\pi(g_{9/2})[404]9/2^+$ orbital. The spin and parity assignments of the bandheads are taken from systematics and are, therefore, tentative. The energies and relative intensities of all of the transitions assigned to ^{117}Cs are given in Table I.

In order to help assign relative spin and parity values to the excited states, a type of gamma-ray angular-distribution measurement was used. Two gamma-gamma correlation matrices were constructed, which were incremented with gamma-ray energies from any germanium detector on one axis, and with gamma-ray energies from detectors at a particular value of θ on the other axis. [In order to increase the number of counts, detectors at θ and $(180\text{-}\theta)°$ were summed.] By gating on the ''any'' germanium detector axis, the intensities of gamma rays detected at θ could be measured in the resulting spectrum. Using this method, the intensities of the gamma rays in the detectors with $\theta \simeq 90°$ I^{90}, (6 detectors), and $\theta \simeq (50 \text{ or } 130)°$ $I^{50/130}$, (34 detectors) were measured, and the ratio $I^{50/130}/I^{90}$ of these intensities was taken (R_{ang}, in Table I). After normalization, the ratio was found to be near 0.7 for a stretched-dipole and near 1.3 for a stretched-quadrupole transition. These values were calibrated using known transitions in the well-studied ^{119}Cs [1] and ^{118}Xe [13] nuclei. Using this method, the relative spin assignments up to $47/2\,\hbar$ in Band 1, $27/2\,\hbar$ in Band 2, and $\sim 27/2\,\hbar$ in Band 3 were made. The values of the measured angular intensity ratios (R_{ang}) are given in Table I, together with the probable multipolarities of the gamma rays.

Assuming that the bands form rotational sequences of stretched E2 transitions, Band 1 extends to $63/2\,\hbar$ (tentatively $71/2\,\hbar$) and Band 2 extends to $51/2\,\hbar$ (tentatively $55/2\,\hbar$). Both Band 1 and Band 2 consist of decoupled sequences of $\Delta I=2$ $E2$ transitions. Two transitions which feed into the $31/2^-$ state of Band 1 may be part of a sideband; however, since their intensity in the present experiment was very low they shall not be considered further. Band 3 consists of two $\Delta I=2$ signature-partner sequences connected by $\Delta I=1$ transitions below about $39/2\,\hbar$. The $\alpha=+1/2$ sequence of Band 3 ($9/2^+$, $13/2^+$ . . .) is observed up to $37/2\,\hbar$ (tentatively $45/2\,\hbar$) and the $\alpha=-1/2$ sequence ($11/2^+$,

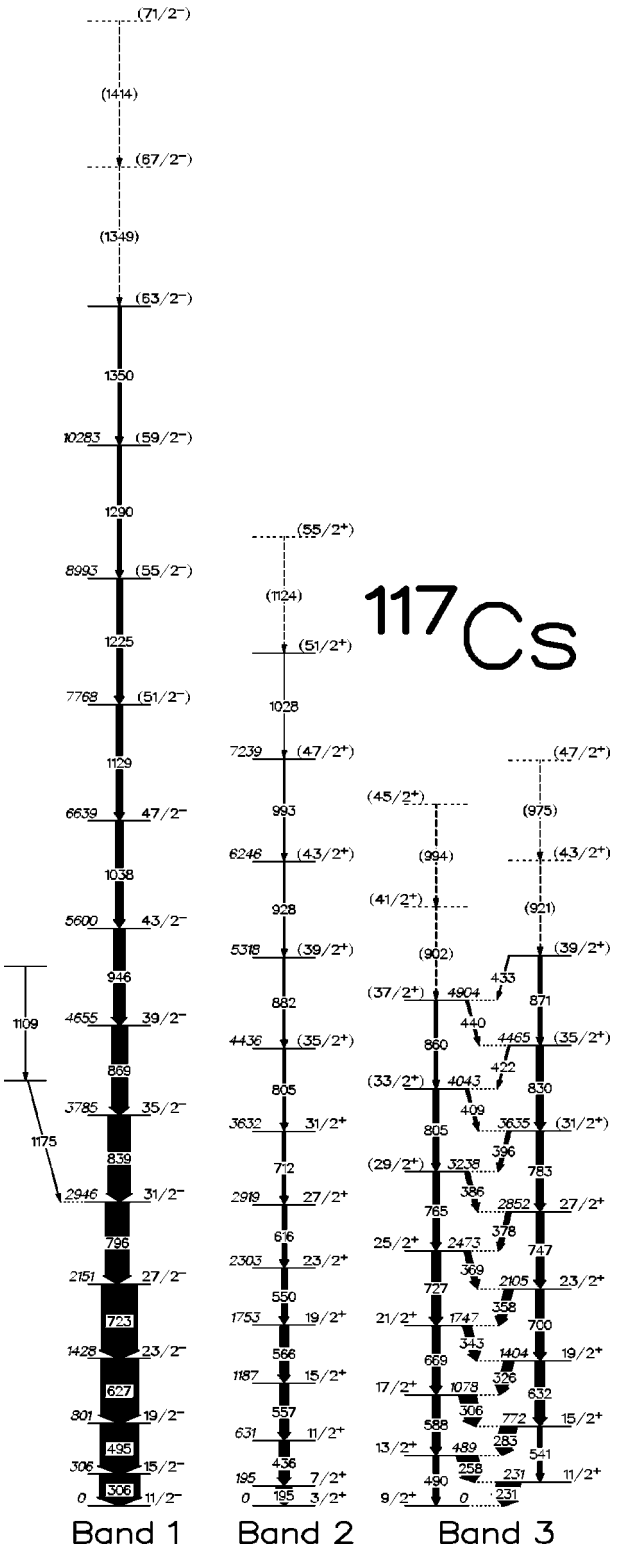

FIG. 5. The level scheme of ^{117}Cs deduced in the present work. The widths of the arrows are approximately proportional to the relative intensities. The level energies and spins given are relative to the respective bandheads. The spins of the bandheads are taken from systematics; all spins given are therefore tentative, but the spins which are not in parentheses are known, relative to the assumed spin of the bandhead. The relative excitation energies of the bands are not known.

TABLE I. Properties of the transitions in ^{117}Cs from the Gammasphere data. Tentative spins are given in parentheses.

E_γ [a]	I_γ [b]	$R_{\rm ang}$	$I_i^{\pi_i} \rightarrow I_f^{\pi_f}$	Band	$\sigma\lambda$
195.2	53(2)	1.16(12)	$\frac{7}{2}^+ \rightarrow \frac{3}{2}^+$	2	$E2$
230.8	75(5)	0.87(9)	$\frac{11}{2}^+ \rightarrow \frac{9}{2}^+$	3	$M1/E2$
257.8	66(5)	0.93(9)	$\frac{13}{2}^+ \rightarrow \frac{11}{2}^+$	3	$M1/E2$
283.1	53(4)	0.92(9)	$\frac{15}{2}^+ \rightarrow \frac{13}{2}^+$	3	$M1/E2$
305.8	40(15)	0.95(10)	$\frac{17}{2}^+ \rightarrow \frac{15}{2}^+$	3	$M1/E2$
306.1	130(16)	1.25(11)	$\frac{15}{2}^- \rightarrow \frac{11}{2}^-$	1	$E2$
326.1	32(2)	0.77(8)	$\frac{19}{2}^+ \rightarrow \frac{17}{2}^+$	3	$M1/E2$
343.2	27(2)	0.90(9)	$\frac{21}{2}^+ \rightarrow \frac{19}{2}^+$	3	$M1/E2$
357.5	28(2)	0.85(9)	$\frac{23}{2}^+ \rightarrow \frac{21}{2}^+$	3	$M1/E2$
368.7	19(1)	0.98(11)	$\frac{25}{2}^+ \rightarrow \frac{23}{2}^+$	3	$M1/E2$
378.5	15(1)	0.69(8)	$\frac{27}{2}^+ \rightarrow \frac{25}{2}^+$	3	$M1/E2$
385.9	14(1)	0.85(10)	$(\frac{29}{2}^+) \rightarrow \frac{27}{2}^+$	3	$M1/E2$
396.5	11(1)		$(\frac{31}{2}^+) \rightarrow (\frac{29}{2}^+)$	3	$M1/E2$
408.8	8(2)		$(\frac{33}{2}^+) \rightarrow (\frac{31}{2}^+)$	3	$M1/E2$
421.7	4(3)	0.74(9)	$(\frac{35}{2}^+) \rightarrow (\frac{33}{2}^+)$	3	$M1/E2$
433.2	2(1)	0.78(9)	$(\frac{39}{2}^+) \rightarrow (\frac{37}{2}^+)$	3	$M1/E2$
435.6	31(1)	1.29(13)	$\frac{11}{2}^+ \rightarrow \frac{7}{2}^+$	2	$E2$
440.2	6(2)		$(\frac{37}{2}^+) \rightarrow (\frac{35}{2}^+)$	3	$M1/E2$
489.7	17(1)		$\frac{13}{2}^+ \rightarrow \frac{9}{2}^+$	3	$E2$
494.8	125(20)	1.23(11)	$\frac{19}{2}^- \rightarrow \frac{15}{2}^-$	1	$E2$
541.2	13(1)	1.53(17)	$\frac{15}{2}^+ \rightarrow \frac{11}{2}^+$	3	$E2$
549.6	18(1)	1.15(12)	$\frac{23}{2}^+ \rightarrow \frac{19}{2}^+$	2	$E2$
556.5	28(1)	1.04(10)	$\frac{15}{2}^+ \rightarrow \frac{11}{2}^+$	2	$E2$
566.1	26(1)	1.20(12)	$\frac{19}{2}^+ \rightarrow \frac{15}{2}^+$	2	$E2$
588.2	25(2)	1.63(18)	$\frac{17}{2}^+ \rightarrow \frac{13}{2}^+$	3	$E2$
616.3	14(1)	1.44(18)	$\frac{27}{2}^+ \rightarrow \frac{23}{2}^+$	2	$E2$
626.9	122(7)	1.34(12)	$\frac{23}{2}^- \rightarrow \frac{19}{2}^-$	1	$E2$
632.3	32(2)	1.49(20)	$\frac{19}{2}^+ \rightarrow \frac{15}{2}^+$	3	$E2$
669.2	26(2)	1.52(17)	$\frac{21}{2}^+ \rightarrow \frac{17}{2}^+$	3	$E2$
699.7	26(2)	1.32(15)	$\frac{23}{2}^+ \rightarrow \frac{19}{2}^+$	3	$E2$
712.2	11(1)		$\frac{31}{2}^+ \rightarrow \frac{27}{2}^+$	2	$E2$
722.8	115(6)	1.57(15)	$\frac{27}{2}^- \rightarrow \frac{23}{2}^-$	1	$E2$
727.2	31(2)		$\frac{25}{2}^+ \rightarrow \frac{21}{2}^+$	3	$E2$
747.4	29(2)		$\frac{27}{2}^+ \rightarrow \frac{23}{2}^+$	3	$E2$
765.1	22(2)	1.52(17)	$(\frac{29}{2}^+) \rightarrow \frac{25}{2}^+$	3	$E2$
783.5	25(2)		$(\frac{31}{2}^+) \rightarrow \frac{27}{2}^+$	3	$E2$
795.7	77(4)	1.47(14)	$\frac{31}{2}^- \rightarrow \frac{27}{2}^-$	1	$E2$
804.8	10(1)		$\frac{35}{2}^+ \rightarrow \frac{31}{2}^+$	2	$E2$
804.8	23(2)		$(\frac{33}{2}^+) \rightarrow (\frac{29}{2}^+)$	3	$E2$
829.9	22(6)		$(\frac{35}{2}^+) \rightarrow (\frac{31}{2}^+)$	3	$E2$
839.2	71(4)	1.21(11)	$\frac{35}{2}^- \rightarrow \frac{31}{2}^-$	1	$E2$
860.5	17(2)		$(\frac{37}{2}^+) \rightarrow (\frac{33}{2}^+)$	3	$E2$
869.1	50(3)	1.44(14)	$\frac{39}{2}^- \rightarrow \frac{35}{2}^-$	1	$E2$
870.9	20(2)		$(\frac{39}{2}^+) \rightarrow (\frac{35}{2}^+)$	3	$E2$
881.8	8(1)		$(\frac{39}{2}^+) \rightarrow (\frac{35}{2}^+)$	2	$E2$
902.2	13(1)		$(\frac{41}{2}^+) \rightarrow (\frac{37}{2}^+)$	3	$E2$
920.8	15(1)		$(\frac{43}{2}^+) \rightarrow (\frac{39}{2}^+)$	3	$E2$

TABLE I. (*Continued*).

E_γ [a]	I_γ [b]	R_{ang}	$I_i^{\pi_i} \rightarrow I_f^{\pi_f}$	Band	$\sigma\lambda$
927.8	5(1)		$(\frac{43}{2}^+) \rightarrow (\frac{39}{2}^+)$	2	$E2$
945.9	37(2)	1.24(13)	$\frac{43}{2}^- \rightarrow \frac{39}{2}^-$	1	$E2$
974.8	8(1)		$(\frac{47}{2}^+) \rightarrow (\frac{43}{2}^+)$	3	$E2$
993.4	4(1)		$(\frac{47}{2}^+) \rightarrow (\frac{43}{2}^+)$	2	$E2$
994.2	10(3)		$(\frac{45}{2}^+) \rightarrow (\frac{41}{2}^+)$	3	$E2$
1027.6	1(1)		$(\frac{51}{2}^+) \rightarrow (\frac{47}{2}^+)$	2	$E2$
1038.4	24(2)	1.34(15)	$\frac{47}{2}^- \rightarrow \frac{43}{2}^-$	1	$E2$
1109 [c]			$(\frac{39}{2}^-)$ [e] $\rightarrow (\frac{35}{2}^-)$ [e]	1	$E2$
1124.3	1(1)		$(\frac{55}{2}^+) \rightarrow (\frac{51}{2}^+)$	2	$E2$
1129.2	20(2)		$(\frac{51}{2}^-) \rightarrow \frac{47}{2}^-$	1	$E2$
1175 [c]			$(\frac{35}{2}^-)$ [e] $\rightarrow \frac{31}{2}^-$	1	$E2$
1224.9	18(2)		$(\frac{55}{2}^-) \rightarrow (\frac{51}{2}^-)$	1	$E2$
1290.1	11(1)		$(\frac{59}{2}^-) \rightarrow (\frac{55}{2}^-)$	1	$E2$
1349	8(4) [d]		$(\frac{67}{2}^-) \rightarrow (\frac{63}{2}^-)$	1	$E2$
1350	10(4) [d]		$(\frac{63}{2}^-) \rightarrow (\frac{59}{2}^-)$	1	$E2$
1413.9	4(1)		$(\frac{71}{2}^-) \rightarrow (\frac{67}{2}^-)$	1	$E2$

[a]Energies typically accurate to 0.2 or 0.3 keV.
[b]Uncertainties on the intensities include a 5% contribution from the efficiency calibration.
[c]Energy estimated, not measured.
[d]Intensity estimated, not measured.
[e]Most likely spin assignment of side-feeding states.

$15/2^+ \ldots$) is observed up to 39/2 $\hbar$ (tentatively 47/2 $\hbar$). The signature splitting is approximately zero over the whole observed rotational frequency range, as would be expected for a band built on a hole in the high-K $\pi(g_{9/2})[404]9/2^+$ orbital.

B. Transmission of residues through the FMA

In order to perform isobaric identification using the method described in Sec. II C, it is essential that a reasonably large fraction of the evaporation residues reach the focal plane of the FMA. In the gamma-gamma ($\gamma\gamma$) coincidence data from the ATLAS/FMA experiment, the three bands shown in Fig. 5 could clearly be seen, with approximately the same relative intensities as in the Gammasphere data, and with Band 1 having the largest relative intensity. In the gamma-gamma data in coincidence with a recoil at the focal plane ($\gamma\gamma$-recoil data) however, it was not possible to observe either Band 1 or Band 2. For this reason, in the present work, only Band 3 can be firmly assigned to ^{117}Cs. The nonobservation of Band 1 and Band 2 in the $\gamma\gamma$-recoil data has been investigated by measuring the intensities of various reaction products in both the $\gamma\gamma$ and $\gamma\gamma$-recoil data, and can be better understood with reference to the data given in Table II. The intensities of bands in ^{116,118}Xe and ^{117,119}Cs have been measured in both an ungated matrix ($I^{\gamma\gamma}$) and in a matrix gated by any recoil ($I^{\gamma\gamma recoil}$).

TABLE II. Intensities of various evaporation residues in the gamma-gamma ($I^{\gamma\gamma}$) and gamma-gamma-recoil ($I^{\gamma\gamma recoil}$) coincidence data. The intensities are given as percentages of the intensity of the yrast band of ^{118}Xe. The uncertainties on the intensities are between 5 and 15 %.

Evap. chan.	Residue/band	$I^{\gamma\gamma}$ (%)	$I^{\gamma\gamma recoil}$ (%)	$I^{\gamma\gamma recoil}/I^{\gamma\gamma}$
$4p$	^{118}Xe/yrast	100	100	1
$\alpha 2p$	^{116}Xe/yrast	37	8	0.22
$3p$	^{119}Cs/$\pi(h_{11/2})$	68	32	0.47
	^{119}Cs/$\pi(g_{7/2})$	10	9	0.90
	^{119}Cs/$\pi(g_{9/2})^{-1}$	40	36	0.90
αp	^{117}Cs/$\pi(h_{11/2})$	2.7	–	–
	^{117}Cs/$\pi(g_{7/2})$	1.1	–	–
	^{117}Cs/$\pi(g_{9/2})^{-1}$	1.5	0.63	0.42

To understand the intensities of Band 1, it is helpful to look at the intensities of the analogous $\pi(h_{11/2})$ band in ^{119}Cs. In the $\gamma\gamma$ data, this band has an intensity of 68% of the ^{118}Xe ($4p$ evaporation) band, but this is reduced to only 32% in the $\gamma\gamma$-recoil data. A possible explanation is that the bandhead of the $\pi(h_{11/2})$ band in ^{119}Cs (and ^{117}Cs) is isomeric, with a lifetime less than the flight time through the FMA (~ 0.7 μs); if the isomer decays within the FMA, the charge state of the recoil is likely to be changed and hence the FMA settings will no longer be appropriate to put the recoils into the ''$M/q=117$'' peak at the focal plane. In the case of ^{117}Cs, the intensity would have to be reduced to $\leqslant 0.5\%$ of the ^{118}Xe band (Table II). This may, therefore, be due to the bandhead being isomeric, with a lifetime of several hundred ns. This does not, however, fully explain the nonobservation of ^{117}Cs Band 1. From the table it can be seen that, in the $\gamma\gamma$ data, the ^{116}Xe ($\alpha 2p$ evaporation) yrast band is observed with 37% of the intensity of the ^{118}Xe yrast band. In the $\gamma\gamma$-recoil data, however, the ^{116}Xe yrast band has only 8% of the intensity of the ^{118}Xe band. This loss of relative intensity has been attributed to the large angular spread of the recoiling evaporation residues, caused by the evaporation of an α particle. The evaporation of an α particle will also reduce the intensities of all three bands in ^{117}Cs (which is produced in the αp evaporation channel) in the $\gamma\gamma$-recoil data, relative to the ^{118}Xe yrast band. This is apparent in the data for Band 3 in ^{117}Cs, where the intensity, relative to ^{118}Xe, is clearly reduced in the $\gamma\gamma$-recoil data (from a comparison with ^{119}Cs, the band head is not expected to be isomeric). This explanation is corroborated by data for two bands in ^{119}Cs ($3p$ evaporation), where the relative intensities are approximately the same in $\gamma\gamma$ and $\gamma\gamma$-recoil data. The reduction of intensity, and hence nonobservation, of ^{117}Cs Band 2 in the $\gamma\gamma$-recoil data can, therefore, be attributed to the angular spread caused by the evaporated α particle. It is also possible that the bandhead of Band 2 is also isomeric.

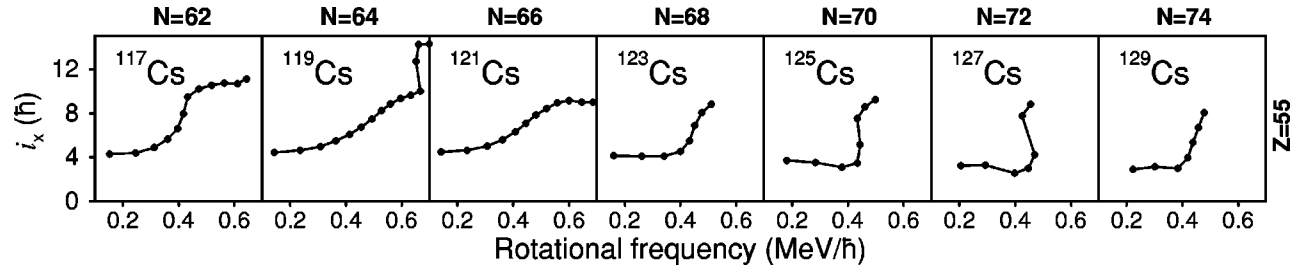

FIG. 6. Systematics of aligned angular momenta in $\pi(h_{11/2})[550]1/2^-$ bands in odd-A $117 \leqslant A \leqslant 129$ cesium isotopes. The data are taken from Refs. [1–5,14] except ^{117}Cs which are from this work. For all data points, a reference configuration has been subtracted with the Harris parameters [20] $\mathcal{J}_0 = 17.0$ MeV$^{-1}\hbar^2$ and $\mathcal{J}_1 = 25.8$ MeV$^{-3}\hbar^4$.

IV. DISCUSSION

A. Assignment of Band 2 to ^{117}Cs

It should be stated explicitly that, although Band 3 has been definitely assigned to ^{117}Cs by this work, and there was some evidence that Band 1 belongs to ^{117}Cs in Ref. [6], there is no direct experimental proof that Band 2 belongs to ^{117}Cs. That being said, there are several facts which strongly suggest that Band 2 does belong to ^{117}Cs. In both the Gammasphere and the ATLAS/FMA data sets, Band 2 is not in coincidence with gamma rays from any known nucleus. In addition, although Band 2 is not observed in the $M = 117$-gated matrix, it is also not observed in any other mass gated matrix with $115 \leqslant M \leqslant 120$. In ^{119}Cs, three bands analogous to those presented here (in ^{117}Cs) are populated with the same relative intensities as the bands in ^{117}Cs; the $\pi(h_{11/2})[550]1/2^-$ band (Band 1) is the most intense, and the $\pi(g_{7/2}d_{5/2})[422]3/2^+$ band (Band 3) is the weakest. Further, it is established that nuclei in this region are well deformed, and that the excitation energies, relative to the bandhead, of the lowest-lying excited states vary smoothly as a function of neutron number [6,15]. The states in Band 2 fit the systematics of the excitation energies of the $\pi[422]3/2^+$ bands very well (as is also apparent from the aligned angular-momentum systematics, discussed below and in Sec. IV B). Finally, a plot of the aligned angular momentum in the $\pi[422]3/2^+$ band is very distinctive and has a characteristic shape caused by a $\pi(h_{11/2})^2$ alignment immediately followed by a $\nu(h_{11/2})^2$ alignment. If the alignment pattern identifies the bandhead as the $\pi[422]3/2^+$ orbital, then the only nuclei to which the band can belong are the odd-Z ^{117}Cs, $^{119}_{57}$La ($p2n$ evaporation), $^{121}_{57}$La (p), $^{115}_{53}$I ($\alpha 3p$), and $^{113}_{53}$I ($2\alpha p$). The level schemes of ^{113,115}I are well known [16,17], essentially ruling them out. The yrast $\pi(h_{11/2})$ band of ^{121}La is known [18], and is not observed in the data. Also, it is unlikely that the $p2n$ channel (^{119}La) is populated in a reaction where neutron evaporation is unfavored. Hence, the most likely candidate is ^{117}Cs.

B. Quasiparticle alignments

The configurations underlying rotational bands can be investigated by studying their aligned angular momenta. In high-spin bands such as those presented in Fig. 5, the aligned angular momenta can easily be extracted according to the standard prescription described in Ref. [19]. The aligned angular momenta (i_x) for the bands in ^{117}Cs are presented as a function of rotational frequency in Figs. 6, 7, and 8; a reference angular momentum has been subtracted with the Harris parameters [20] $\mathcal{J}_0 = 17.0$ MeV$^{-1}\hbar^2$ and $\mathcal{J}_1 = 25.8$ MeV$^{-3}\hbar^4$ [21]. By comparing the experimental alignments with those predicted theoretically, and by applying Pauli blocking arguments, information about the underlying configurations can be obtained. In this work, the standard procedure has been adopted, whereby total Routhian surface (TRS) [22,23] calculations are used to estimate the deformations of the proposed configurations, and these deformations are subsequently used as input into Woods-Saxon cranked shell model calculations [24,25] in order to extract theoretical quasiparticle alignment frequencies. These calculated alignment frequencies can then be compared to those observed experimentally.

In order to facilitate the discussion of the bands, the orbitals are labeled as indicated in Table III. The TRS calculations predict axially-symmetric shapes for both the lowest positive-parity (a and b) and the lowest negative-parity (e and f) configurations in ^{117}Cs. At a representative rotational frequency of $\omega = 0.190$ MeV/$\hbar$, the lowest positive-parity, negative-signature configuration (b configuration) is pre-

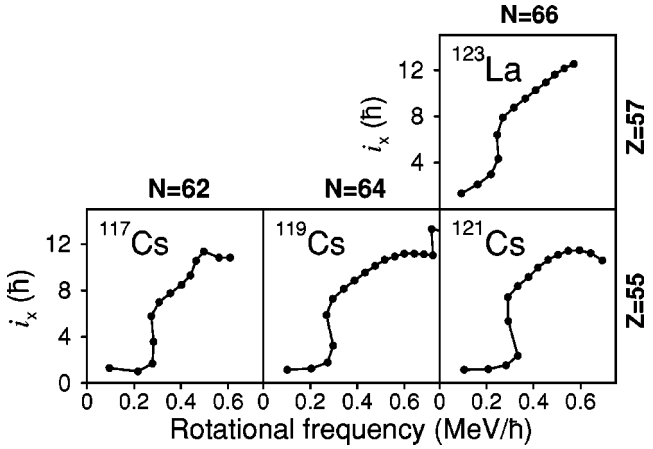

FIG. 7. Systematics of aligned angular momenta in the $\pi(g_{7/2}d_{5/2})[422]3/2^+$ bands of ^{117,119,121}Cs and ^{123}La. The data are taken from Refs. [1,14,26] except ^{117}Cs which are from this work. For all data points, a reference configuration has been subtracted with the Harris parameters [20] $\mathcal{J}_0 = 17.0$ MeV$^{-1}\hbar^2$ and $\mathcal{J}_1 = 25.8$ MeV$^{-3}\hbar^4$.

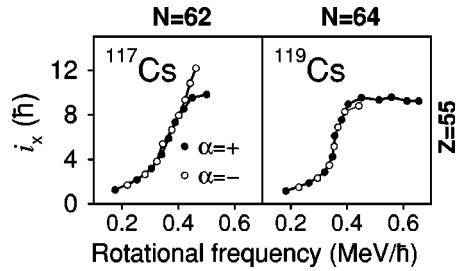

FIG. 8. Aligned angular momenta in the $\pi(g_{9/2})^{-1}[404]9/2^+$ bands of ^{117,119}Cs. The data for ^{119}Cs are taken from Refs. [1,14] and those for ^{117}Cs are from this work. For all data points, a reference configuration has been subtracted with the Harris parameters [20] $\mathcal{J}_0=17.0$ MeV$^{-1}\hbar^2$ and $\mathcal{J}_1=25.8$ MeV$^{-3}\hbar^4$.

dicted to have a deformation of $\beta_2=0.251$, $\beta_4=0.044$, and $\gamma=3.9°$; at the same rotational frequency, the lowest negative-parity, negative-signature configuration (*e* configuration) has a deformation of $\beta_2=0.239$, $\beta_4=0.036$, and $\gamma=-0.7°$. It should be pointed out, however, that the TRS calculations for the positive-parity configurations are of limited reliability due to configuration mixing, and the existence of positive-parity orbitals from below the $Z=50$ shell gap. The positive-parity TRS surfaces in this region consist of a mixture of the $[404]9/2^+$, $[422]3/2^+$, and $[420]1/2^+$ orbitals. Performing cranked Woods-Saxon calculations over a reasonable range of deformations, however, reveals that the calculated alignment frequencies do not vary significantly with deformation, as is illustrated in Fig. 9. For this reason, the alignment frequencies of the same pair of nucleons in the three ^{117}Cs bands should be very nearly the same. At the representative deformation of $\beta_2=0.25$, $\beta_4=0.04$, and $\gamma=0°$, the cranking calculations predict the alignments of $h_{11/2}$ neutrons and protons at the frequencies given in Table IV.

1. Band 1

Only one signature of the Band 1 is observed, which indicates large signature splitting, characteristic of a low-*K* orbital. The aligned angular momentum of Band 1 is shown in the left-most panel of Fig. 6 as a function of rotational frequency. The band has a large initial alignment of $i_x=4.5$ $\hbar$, suggesting that the band is based on an $h_{11/2}$ orbital. The most likely candidate is then the $[550]1/2^-$ Nilsson orbital. This would agree with the systematics of the neighboring odd-*A* cesium isotopes which suggest that the

TABLE III. Labeling scheme for orbitals near the Fermi surface.

Label		Parity	Signature
neutrons	protons	(π)	(α)
A, C	a, c	+	+1/2
B, D	b, d	+	−1/2
E, G	e, g	−	−1/2
F, H	f, h	−	+1/2

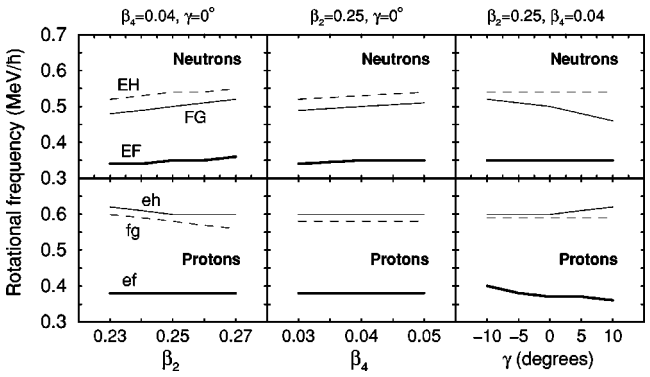

FIG. 9. Calculated alignment frequencies of the lowest three pairs of $h_{11/2}$ neutrons (upper panels) and protons (lower panels), as a function of the deformation parameters β_2, β_4, and γ. Values of the deformation parameters which were not varied are given above the panels.

lowest state in the band has spin and parity of $11/2^-$. The first upbend in the alignment plot is observed at 0.40 MeV/$\hbar$. This is close to the theoretically predicted value for the first $(h_{11/2})^2$ neutron alignment (EF), and infers that the first $(h_{11/2})^2$ proton alignment (ef) is blocked. These observations suggest that the band is based on an $h_{11/2}$ proton orbital. The upbend at 0.40 MeV/$\hbar$ is therefore attributed to the alignment of the first pair of $h_{11/2}$ neutrons (EF). The increase in i_x for the highest data point in ^{117}Cs (Fig. 6) may be due to the onset of the alignment of the first nonblocked $h_{11/2}$ proton pair (fg), although more data are clearly needed to help elucidate this assignment.

2. Band 2

A plot of the aligned angular momentum in Band 2 is given in the left-most panel of Fig. 7. Again, only one signature partner of the band is observed, which indicates that it is based on a low-*K* orbital with large signature splitting. The two candidate Nilsson orbitals near the Fermi surface would then be the $g_{7/2}/d_{5/2}$ $[422]3/2^+$ and $[420]1/2^+$ orbitals. Calculated Routhians predict that the $[422]3/2^+$ band lies slightly lower in energy than the $[420]1/2^+$ band and thus it is likely that the bandhead of Band 2 is the $3/2^+$ state of the $[422]3/2^+$ band. The assignment as a $[420]1/2^+$ band, however, cannot be ruled out, since there is no way to distinguish between bands based on these two orbitals from the present data.

TABLE IV. Alignment frequencies of pairs of $h_{11/2}$ neutrons and protons in ^{117}Cs, as predicted by cranked Woods-Saxon calculations. The alignments of positive-parity quasiparticles are predicted at frequencies above 0.7 MeV/$\hbar$, and are therefore not considered here.

neutrons	ω_c (MeV/$\hbar$)	protons	ω_c (MeV/$\hbar$)
EF	0.35	ef	0.38
FG	0.50	fg	0.60
EH	0.55	eh	0.58

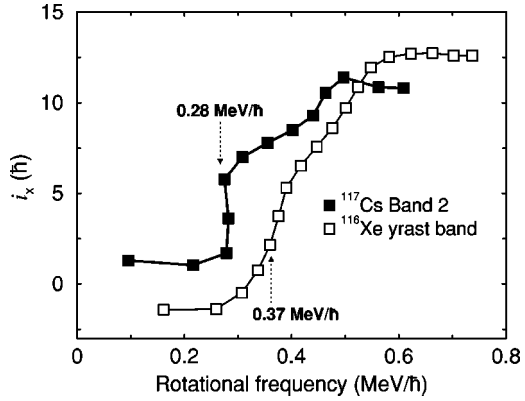

FIG. 10. Comparison of the aligned angular momentum of Band 2 of ^{117}Cs with that of the yrast band of ^{116}Xe [13]. The numbers in bold text give the alignment frequencies of the first $(h_{11/2})^2$ proton alignment in the bands. For all data points, a reference configuration has been subtracted with the Harris parameters [20] $\mathcal{J}_0 = 17.0\ \mathrm{MeV}^{-1}\hbar^2$ and $\mathcal{J}_1 = 25.8\ \mathrm{MeV}^{-3}\hbar^4$.

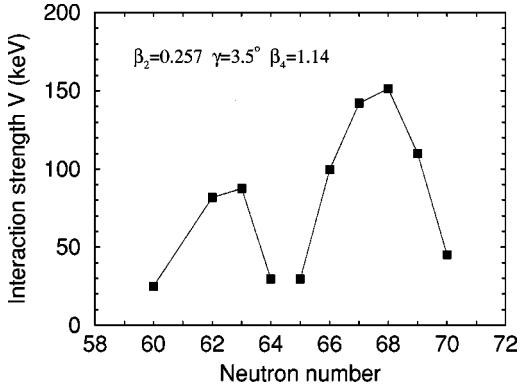

FIG. 11. Calculated interaction strengths for the $(h_{11/2})^2$ neutron alignments in the cesium isotopes with $60 \leqslant N \leqslant 70$. The values are taken from Ref. [1] where calculations were made at the deformation given on the figure.

If the $[422]3/2^+$ (or $[420]1/2^+$) assignment is correct, then neither the first $h_{11/2}$ proton nor the first $h_{11/2}$ neutron alignment will be blocked and both alignments should be observed in the band. Inspection of Fig. 7 reveals that there is a sharp gain in i_x (backbend) at $\omega = 0.28$ MeV/$\hbar$, followed by a more gradual gain in i_x (upbend) centered at about 0.38 MeV/$\hbar$. The gradient and frequency of the upbend at 0.38 MeV/$\hbar$ is very similar to the upbend in Band 1, where the first $\pi(h_{11/2})^2$ (ef) alignment is blocked; this upbend is therefore attributed to the alignment of the first pair of $h_{11/2}$ neutrons (EF). The alignment at 0.28 MeV/$\hbar$ is consequently due to the first pair of $h_{11/2}$ protons (ef). The total alignment gain measured over the frequency range seen in the experiment is consistent with this interpretation.

3. Band 3

Band 3 is strongly coupled and is therefore based on an orbital with a high-K value. The only nearby possibility is the $\pi(g_{9/2})[404]9/2^+$ Nilsson orbital which would give the bandhead a spin and parity of $9/2^+$; this assignment is in agreement with systematics. The aligned angular momentum of the band is presented in Fig. 8, in comparison to the analogous band in ^{119}Cs. The bands in both nuclei display very similar alignment patterns, centered around 0.38–0.40 MeV/$\hbar$ and with a total alignment gain of about 9 $\hbar$. This alignment gain is attributed to the near-superposition of the $(h_{11/2})^2$ proton alignment (ef) at 0.36 MeV/$\hbar$ and the $(h_{11/2})^2$ neutron alignment (EF) at 0.40 MeV/$\hbar$. Moreover, the total alignment gain is approximately equal to that in Band 2 (Fig. 7), where the same two alignments occur, but at slightly different frequencies.

C. The $\pi(h_{11/2})^2$ alignment in Bands 2 and 3

The first $h_{11/2}$ proton alignment (ef) is observed in both Bands 2 and 3. In Band 2, the observed alignment frequency, 0.28 MeV/$\hbar$, is considerably lower than both the calculated frequency of 0.38 MeV/$\hbar$ (Table IV) and the alignment observed in the even-even core ^{116}Xe, as shown in Fig. 10. This effect in Bands 2 and 3 was also observed in the analogous band in ^{123}La [26], where it was attributed to a pairing effect due to the blocking of an extra orbital in the odd-Z nuclei, resulting in a reduction of the proton pair gap. The same effect has been documented previously in the heavier rare-earth nuclei [27].

In calculations performed in Ref. [26] (details therein), the proton pair gap was found to be 25% lower in ^{123}La as compared to the even-even ^{122}Ba core. In that work, this was given as the reason why the frequency of the $\pi(h_{11/2})^2$ alignment in ^{123}La was reduced. The results presented here for ^{117}Cs are analogous to the observations in ^{123}La; however, the discussion presented in Sec. IV E suggests that a neutron-proton interaction influences the alignment frequencies.

D. The $\nu(h_{11/2})^2$ alignment in Band 1

The aligned angular momenta in the $\pi(h_{11/2})[550]1/2^-$ bands of the odd-A cesium isotopes with $117 \leqslant A \leqslant 129$ are shown in Fig. 6, as a function of rotational frequency. As pointed out in Ref. [1], the deformation for this configuration is predicted to be stable as a function of N, and deformation effects on the aligned angular momentum are small. The strength of the interaction at the $(h_{11/2})^2$ neutron alignment is predicted to be an oscillating function of the neutron number with a large value for ^{123}Cs ($N = 68$) and small values for ^{119}Cs ($N = 64$) and ^{125}Cs ($N = 70$). The calculated interaction strengths, taken from Ref. [1], are shown in Fig. 11; the calculations are made at a representative deformation, given on the figure. Experimentally, the strength of an interaction can be inferred from a plot of aligned angular momentum against rotational frequency, where a sharp backbend implies a weak interaction and a gradual upbend implies a strong interaction. Inspection of Fig. 6 gives an immediate comparative estimate of the interaction strengths at the $(h_{11/2})^2$ neutron alignments in $^{117-129}$Cs. As predicted by the calculations, the interaction strength in ^{125}Cs appears to be small. Contrary to the calculations, however, the interaction strength appears to continually increase with decreasing neutron number down to ^{119}Cs. In Ref. [1], this was ascribed to

a residual neutron-proton interaction between the valence protons and the aligning neutrons. For ^{117}Cs, the interaction strength is lower than in ^{119}Cs, as can be inferred from Fig. 6. It would appear that the interaction strength does oscillate, but with a maximum at $N=64-66$ rather than at $N=68$ which was predicted by standard cranking calculations.

E. Implications of a neutron-proton interaction

It is apparent from the discussion given in the previous subsections that the alignment frequencies have a dependence on the configurations of the rotational bands in which they occur, and also that there are several discrepancies between the observed frequencies and those predicted using the standard CSM. This failure of the CSM to match all of the features of an alignment is not a new observation. It is well established that systematic discrepancies are encountered when trying to reproduce alignment patterns of high-spin states, particularly in bands based on intruder orbitals [28]. For the neutron-deficient cesium isotopes the aligning $h_{11/2}$ neutrons and protons are in nearly the same $h_{11/2}$ orbitals as the protons upon which bands are based. This suggests that a neutron-proton (np) interaction may need to be considered. An np interaction is not included in the standard CSM; in order to investigate its role, Satula, Wyss, and Dönau [29] have performed calculations using an approach similar to the standard cranking method, but which is supplemented with additional mixing effects arising from a residual np interaction. In their work, the np interaction is assumed to be a quadrupole-quadrupole (qq) force. Despite this admitted simplification, the results of the calculations qualitatively explain some of the discrepancies between CSM theory and experimental observations. Although, specifically, the calculations were performed for ^{113}Sb, several of the general conclusions can be applied to ^{117}Cs, an isotone of ^{113}Sb.

The calculations reveal the manner in which the np interaction can shift alignment frequencies. When particles align within an intruder subshell, the alignment frequency is shifted up if the aligning particles already occupy intruder orbitals, and down if the aligning particles occupy normal-parity orbitals. The reason for this effect is that intruder orbitals have large intrinsic quadrupole moments; their occupation can modify the quadrupole moment of the system and, hence, change the qq force. In the preceding subsections, it was stated that, in ^{117}Cs, the first $(h_{11/2})^2$ neutron alignments (EF) occur at frequencies of 0.40, 0.38, and 0.40 MeV/$\hbar$ in Bands 1, 2, and 3, respectively. Theoretically, this alignment is predicted by the standard CSM to occur at 0.35 MeV/$\hbar$ (see Table IV and Fig. 6). In ^{117}Cs, the neutron Fermi level lies approximately at the $[532]5/2^-$ orbital. Therefore, before the $\nu(h_{11/2})^2$ alignment occurs, the aligning neutrons already occupy $h_{11/2}$ orbitals, and the alignment reduces the quadrupole moment (see Fig. 8 of Ref. [29]). As a consequence, the qq interaction is also reduced, the two quasineutron band lies at higher energy, and the alignment is shifted to higher frequency. In Band 2, the $\pi(h_{11/2})^2$ (ef) alignment occurs at 0.28 MeV/$\hbar$, compared with a CSM-predicted value of 0.38 MeV/$\hbar$. The low frequency of this alignment can also be explained in a similarly qualitative manner. In ^{117}Cs, the proton Fermi level lies at the $[550]1/2^-$ orbital, and in Band 2 the valence proton occupies either the $[422]3/2^+$ or $[420]1/2^+$ normal-parity orbital. Following the $\pi(h_{11/2})^2$ alignment, two protons occupy $h_{11/2}$ orbitals. The quadrupole moment and also therefore the qq interaction is increased, the energy of the two quasiproton band is reduced, and the alignment is shifted to a lower frequency. In Ref. [29], it is stated that the effect of the np interaction is largest when the Fermi level is low in the intruder subshell. Hence, the frequency of the $\pi(h_{11/2})^2$ alignment in Band 2 is reduced markedly. (Alignment frequencies in Band 3 are difficult to pinpoint and are, therefore, not discussed here.)

It is also expected that an np interaction will perturb the interaction strengths. From the present data, the behavior of the interaction strengths is puzzling. As stated in Sec. IV D, it appears that the local maximum of the interaction strength occurs at $N\simeq 64$, rather than the value of $N\simeq 68$ which was predicted by the CSM. However, in Ref. [29], the inclusion of the np interaction shifts the theoretical maximum to higher N. Clearly, further theoretical investigation is necessary before the role of the np interaction on quasiparticle alignments in odd-A nuclei is fully understood.

V. SUMMARY

High-spin states have been populated in the very neutron-deficient ^{117}Cs isotope, and studied using the Gammasphere array. For the first time, excited states have been identified in the $\pi(g_{9/2})^{-1}$ band using a method of gamma-recoil and gamma-x ray coincidences. The $\pi(h_{11/2})$ band has been observed and extended to high spin. A third band, presumably based on a $\pi(g_{7/2}d_{5/2})$ orbital has been tentatively assigned to ^{117}Cs, primarily on the basis of excitation-energy and alignment systematics. There is some indirect, tentative evidence that the $\pi(h_{11/2})$ bandhead is isomeric with a halflife of several hundred ns. Alignments of both $h_{11/2}$ neutrons and protons are observed in all of the bands. Like in the neighboring heavier cesium isotopes, the $\pi(h_{11/2})^2$ alignment in the $\pi(g_{7/2}d_{5/2})$ band occurs at a frequency lower than the prediction of the standard CSM. The interaction strength at the $(h_{11/2})^2$ neutron alignment in the $\pi(h_{11/2})$ band appears to be smaller than that in ^{119}Cs. Though the behavior of the quasiparticle alignment frequencies is hard to explain with the standard CSM, it appears that the behavior can be better qualitatively described if a neutron-proton interaction is taken into consideration.

ACKNOWLEDGMENTS

Targets were prepared by A. Lipski (Stony Brook). The authors would like to acknowledge useful suggestions from R. Wyss. The CSM and TRS codes were provided by R. Wyss and W. Nazarewicz. This work is supported in part by the NSF, the EPSRC (UK), and by the Department of Energy, Nuclear Physics Division, under Contracts No. W-31-109-ENG-38 (ANL) and DE-AC03-76SF00098 (LBNL).

[1] F. Lidén *et al.*, Nucl. Phys. **A550**, 365 (1992).
[2] J. R. Hughes, D. B. Fossan, D. R. LaFosse, Y. Liang, P. Vaska, M. P. Waring, and J.-y. Zhang, Phys. Rev. C **45**, 2177 (1992).
[3] J. R. Hughes, D. B. Fossan, D. R. LaFosse, Y. Liang, P. Vaska, and M. P. Waring, Phys. Rev. C **44**, 2390 (1991).
[4] Y. Liang, R. Ma, E. S. Paul, N. Xu, D. B. Fossan, and R. A. Wyss, Phys. Rev. C **42**, 890 (1990).
[5] L. Hildingsson *et al.*, Z. Phys. A **340**, 29 (1991).
[6] X. Sun *et al.*, Phys. Rev. C **51**, 2803 (1995).
[7] C. J. Gross *et al.*, in *ENAM98: Exotic Nuclei and Atomic Masses*, edited by B. M. Sherrill, D. J. Morrissey, and C. N. Davids, AIP Conf. Proc. No. 455 (AIP, New York, 1998), p. 444.
[8] P. J. Nolan, F. A. Beck, and D. B. Fossan, Annu. Rev. Nucl. Part. Sci. **44**, 561 (1994).
[9] C. N. Davids *et al.*, Nucl. Instrum. Methods Phys. Res. B **40/41**, 1224 (1989); **70**, 358 (1991).
[10] J. F. Smith *et al.*, Phys. Lett. B **406**, 7 (1997).
[11] J. F. Smith *et al.*, Phys. Rev. C **57**, R1037 (1998).
[12] D. C. Radford, Nucl. Instrum. Methods Phys. Res. A **361**, 297 (1995); **361**, 306 (1995).
[13] J. M. Sears, D. B. Fossan, G. R. Gluckman, J. F. Smith, I. Thorslund, E. S. Paul, I. M. Hibbert, and R. Wadsworth, Phys. Rev. C **57**, 2991 (1998).
[14] R. Wadsworth *et al.* (unpublished).
[15] J. F. Smith *et al.*, Phys. Rev. C **61**, 044329 (2000).
[16] M. P. Waring *et al.*, Phys. Rev. C **51**, 2427 (1995).
[17] E. S. Paul *et al.*, J. Phys. G **18**, 837 (1992); E. S. Paul *et al.*, Phys. Rev. C **50**, 741 (1994).
[18] B. Cederwall, A. Johnson, B. Fant, S. Juutinen, P. Ahonen, S. Miterai, J. Mukai, and J. Nyberg, Z. Phys. A **338**, 463 (1991).
[19] R. Bengtsson and S. Frauendorf, Nucl. Phys. **A327**, 139 (1979).
[20] S. M. Harris, Phys. Rev. **138**, B509 (1965).
[21] D. M. Todd, R. Aryaeinejad, D. J. G. Love, A. H. Nelson, P. J. Nolan, P. J. Smith, and P. J. Twin, J. Phys. G **10**, 1407 (1984).
[22] R. Wyss, J. Nyberg, A. Johnson, R. Bengtsson, and W. Nazarewicz, Phys. Lett. B **215**, 211 (1989).
[23] W. Nazarewicz, G. A. Leander, and A. Johnson, Nucl. Phys. **A503**, 285 (1989).
[24] W. Nazarewicz, J. Dudek, R. Bengtsson, and I. Ragnarsson, Nucl. Phys. **A435**, 397 (1985).
[25] S. Cwiok, J. Dudek, W. Nazarewicz, W. Skalski, and T. Werner, Comput. Phys. Commun. **46**, 379 (1987).
[26] R. Wyss *et al.*, Nucl. Phys. **A503**, 244 (1989).
[27] J. D. Garrett *et al.*, Phys. Rev. Lett. **47**, 75 (1981).
[28] R. Wyss and A. Johnson, in *Proceedings of the International Conference on High-Spin Physics*, edited by J. X. Saladin, R. A. Sorenson, and C. M. Vincent (World Scientific, Singapore, 1991), p. 123.
[29] W. Satula, R. Wyss, and F. Dönau, Nucl. Phys. **A565**, 573 (1993).